Vacuum-Ultraviolet Photoionization and Mass Spectrometric Characterization of Lignin Monomers Coniferyl and Sinapyl Alcohols

Lynelle K. Takahashi,[1, 2] Jia Zhou,[1] Oleg Kostko,[1] Amir Golan,[1] Stephen R. Leone,[1, 2, 3] and Musahid Ahmed[1,*]

[1]*Chemical Sciences Division, Lawrence Berkeley National Laboratory, Berkeley, CA 94720*

[2]*Department of Chemistry, University of California at Berkeley, Berkeley, CA 94720*

[3]*Department of Physics, University of California at Berkeley, Berkeley, CA 94720*

* Corresponding author: MS: 6R-2100, Lawrence Berkeley National Laboratory, 1 Cyclotron Road,

Berkeley, CA 94720, USA. Phone: (510) 486-6355; fax: (510) 486-5311; e-mail: MAhmed@lbl.gov

Abstract

The fragmentation mechanisms of monolignols under various energetic processes are studied with jet-cooled thermal desorption molecular beam (TDMB) mass spectrometry (MS), 25 keV Bi_3^+ secondary ion MS (SIMS), synchrotron vacuum-ultraviolet secondary neutral MS (VUV-SNMS) and theoretical methods. Experimental and calculated appearance energies of fragments observed in TDMB MS indicate that the coniferyl alcohol photoionization mass spectra contain the molecular parent and several dissociative photoionization products. Similar results obtained for sinapyl alcohol are also discussed briefly. Ionization energies of 7.60 eV ± 0.05 eV for coniferyl alcohol and <7.4 eV for both sinapyl and dihydrosinapyl alcohols are determined. The positive ion SIMS spectrum of coniferyl alcohol shares few characteristic peaks (m/z = 137 and 151) with the TDMB mass spectra, shows extensive fragmentation, and does not exhibit clear molecular parent signals. VUV-SNMS spectra, on the other hand, are dominated by the parent ion and main fragments also present in the TDMB spectra. Molecular fragmentation in VUV-SNMS spectra can be reduced by increasing the extraction delay time. Some features resembling the SIMS spectra are also observed in the desorbed neutral products. The monolignol VUV-SNMS peaks shared with the TDMB mass spectra suggest that dissociative photoionization of ion-sputtered neutral molecules predominate in the VUV-SNMS mass spectra, despite the extra internal energy imparted in the initial ion impact. The potential applications of these results to imaging mass spectrometry of bio-molecules are discussed.

Keywords: secondary neutral mass spectrometry, secondary ion mass spectrometry, monolignols, coniferyl alcohol, sinapyl alcohol, photoionization, fragmentation

Introduction

Lignin is the second most abundant, naturally occurring biopolymer on Earth. Its close association with cellulose in plant cell walls contributes to plants' structural integrity and resistance to pathogens.[1] While these qualities are valuable for plant survival and thereby make studies of lignocellulosic systems fundamentally important, lignin also has broad economic significance. It is a major hindrance in the production of pulp for paper[2] and, more recently, to the rapid conversion of plant materials into monomer sugars and alcohol biofuels.[3] For these reasons, lignin and lignocellulosic materials are active fields of research.[3-5]

Many techniques have been implemented to analyze the chemical makeup of biomass.[6] In particular, a number of mass spectrometry (MS) methods have been used to study lignin, [7] including pyrolysis gas chromatography MS and pyrolysis MS,[8] both of which can utilize electron ionization (EI). Single photon ionization time-of-flight MS has also been applied recently to biomass studies,[9] simplifying the mass spectral signatures of lignin degradation products by depositing less energy into the analyte mixture.

The simplification of mass spectral signatures is also desirable in studies involving chemical imaging of lignin within biomass. In secondary ion MS (SIMS) analyses of wood,[10] the characteristic fragments from guaiacyl and syringyl lignin[11,12] have been used to map the chemical composition of wood in its native state. While SIMS is desirable due to its high spatial resolution, its molecular specificity, and the minimal sample preparation required, SIMS spectra of chemically heterogeneous systems are notoriously complicated, and secondary ion signals are often strongly affected by the local chemical environment.[13] SIMS images are therefore non-quantitative and difficult to interpret. It would be advantageous to minimize fragmentation observed with SIMS.

Secondary neutral MS (SNMS) is an alternative to SIMS, and it has been shown to give more quantitative results since the desorption yield of neutrals is less susceptible to the local chemical environment.[13] In SNMS the desorbed neutral analyte molecules must be ionized before analysis. EI has been used for many decades to ionize gas-phase neutrals; however it is often a "hard" ionization technique that can heavily fragment fragile organic molecules found in biological systems.[14] Postionization with laser systems has also been explored,[15,16] but organic molecules ionize in a photon energy region where

tunable radiation is difficult to obtain. Multiphoton ionization techniques have been used,[17] but considerable molecular fragmentation results from the excessive energy imparted during the ionization process.

Recently, femtosecond mid-IR lasers have been applied to ionize organic molecules sputtered by 40 keV C_{60}^{+}.[18] It was found that the sensitivity for the molecular parent ions of various molecules could be improved using tunnel ionization with high peak power, long-wavelength laser fields. Ionization with longer-wavelength, 1450 nm laser radiation was found to greatly reduce molecular fragmentation compared to ionization with 800 nm laser radiation.

An alternative to the aforementioned ionization methods is single-photon, near-threshold ionization using wavelength-tunable synchrotron vacuum-ultraviolet (VUV) radiation. This method has been shown to ionize gas-phase organic molecules with minimal fragmentation[19] as well as provide quantitative information on molecular energies. In some cases, synchrotron VUV has aided in the identification of compounds on the basis of their ionization energies (IEs).[20] Single photon ionization has also been used to monitor lignin decomposition products with varying temperature.[9,21] Recently, VUV threshold ionization has been applied to study ion-sputtered neutral inorganic clusters and organic molecules in VUV-SNMS, where it has been shown to simplify mass spectra[22] and provide information on the internal energies of ion-sputtered neutrals.[23]

In this paper, threshold single photon ionization is applied to study the photoionization of coniferyl alcohol and sinapyl alcohol, two monomer units of lignin (Figure 1).[24] The monolignols are introduced into a thermal desorption molecular beam (TDMB) to study the energetics and fragmentation pathways of cold monolignol molecules. Mass spectra of coniferyl and sinapyl alcohol ionized at various near-threshold energies are presented, and fragment appearance energies (AEs) are used together with theoretical values to evaluate the fragmentation mechanisms. TDMB mass spectra of coniferyl alcohol are compared to the corresponding SIMS and VUV-SNMS spectra in detail, and sinapyl alcohol is also briefly discussed. The origins of fragments in the VUV-SNMS spectra are discussed to evaluate the application of near-threshold ionization techniques to ion-probe MS imaging studies of lignin.

Experimental

Coniferyl and sinapyl alcohol mass spectra are collected using three methods. In TDMB mass spectra, monolignols are introduced into the gas phase by thermally desorbing and cooling them in a supersonic

expansion. These low-internal energy gas phase molecules are ionized with wavelength-tunable VUV photons to gain intuition for dissociative photoionization pathways. The TDMB spectra are compared to positive ion SIMS and VUV-SNMS mass spectra collected using a 25 keV Bi_3^+ ion probe for desorption. SIMS mass spectra probe the secondary cations that are sputtered and ionized with the primary Bi_3^+ ion impact. In VUV-SNMS, high-internal-energy neutrals sputtered by the Bi_3^+ ion beam are probed by VUV photoionization. VUV-SNMS is compared to TDMB and SIMS mass spectra to distinguish between the fragmentation induced by the primary ion and the ionizing photon.

Thermal Desorption Molecular Beam with VUV Photoionization

Analysis of thermally vaporized monolignols in a molecular beam is performed in a home-built reflectron-type mass spectrometer that has been previously used in photoionization studies of laser ablated species.[25] The instrument is adapted for the photoionization of monolignols by using a thermally heated nozzle described in detail in a previous study of hydrated DNA bases.[26]

Very briefly, ~50 mg of solid coniferyl alcohol (98% purity, Alfa Aesar and Sigma Aldrich) or sinapyl alcohol (80% purity, Sigma Aldrich) are introduced, without further purification, directly into a stainless steel cylindrical nozzle with a 100 µm-diameter aperture. The tip of the nozzle, where the compound is introduced, is heated with a cartridge heater, and the thermally vaporized monolignols are carried by 145 Torr (19.3 kPa) of argon into the source chamber. A 2 mm-diameter skimmer separates the source chamber from the photoionization region. The ionized molecules are ionized with the VUV beam of the synchrotron and are extracted into a perpendicularly configured reflectron-type time-of-flight mass spectrometer, and the mass spectrum is recorded using software written with LabVIEW. The nozzle is cleaned between compounds by thoroughly rinsing with methanol, ethanol, and acetone. Although there is no direct measure of the temperature of the molecular beam, the experimental conditions in the TDMB experiments are similar to the 150 µm diameter nozzle and 175 Torr (23.3 kPa) Ar backing pressure used by Amirav et al.,[27] who suggest temperatures of ≈7 K for rotations and <50 K for vibrations for molecules with similar molecular weights.

The ionizing VUV radiation is provided by the 10-cm period undulator of the Chemical Dynamics Beamline at the Advanced Light Source, Lawrence Berkeley National Laboratory. The radiation is quasi-continuous (70 ps pulses at 500 MHz).[28] The synchrotron was recently upgraded to operate in top-off mode,[29] increasing the photon flux available to each beamline. Higher harmonic radiation is filtered by passing the radiation through a gas filter. Argon or krypton gas is used in the filter, depending on the

spectral energy range that is being examined. The resulting synchrotron radiation is reflected from a 3-meter monochromator with a 1 mm-horizontal exit slit. The monochromatized light reaches the ionization region with a spectral resolution of ~50 meV and a flux of ~10^{14} photons per second.[30]

In some of the TDMB mass spectra presented below, argon ions are observed below the threshold photon energy for their ionization. This has been observed before in other experiments at the beamline, and it is attributed to ionization by the residual higher harmonic radiation that passes the gas filter.[31]

The nozzle temperature is increased while monitoring the monolignol signal at 11 eV photon energy until a satisfactory signal level is obtained for the collection of photoionization efficiency (PIE) curves for the parent molecules. Several datasets are taken as the photon energy is scanned, either in 0.2 eV steps for coarse scans over a large photon energy range or 0.05 eV steps for fine scans over smaller energy ranges. Mass spectra from $3x10^5$ time-of-flight cycles are summed for each photon energy data point. Photon flux curves for normalization of collected PIE curves are determined using a NIST-calibrated photodiode (SXUV-100, International Radiation Detectors) attached near the light exit port.

Secondary Ion and VUV-Secondary Neutral Mass Spectrometry (SIMS / VUV-SNMS)

A modified commercial reflectron-type time-of-flight secondary ion mass spectrometer (TOF.SIMS V; IonTOF, Germany) is coupled to a non-monochromatized synchrotron VUV light port on the same beamline. Mass-selected Bi_3^+ ions with 25 keV kinetic energy impact the sample surface at 45°, ejecting cationic, anionic, and neutral chemical species. Unless otherwise noted, SIMS spectra are acquired with 12.5 ns Bi_3^+ pulses over an area of 150 μm x 150 μm, with a 64 pixel x 64 pixel raster scan at a repetition rate of 10 kHz, and secondary ions are extracted with a 10 μs long, -2000 V pulse.

The VUV-SNMS analysis of the monolignol samples is performed using the TOF.SIMS V instrument over the same sample location as the SIMS analysis, with the same 64 pixel x 64 pixel raster scan. Due to the limited photon flux used for photoionization, VUV-SNMS signals are significantly weaker than the corresponding SIMS signals, so the spectra of the photoionized neutrals are collected using longer pulses of Bi_3^+ that span 50 ns. Datasets used for the VUV-SNMS PIE curves presented below are collected over the same location on the sample.

For the VUV-SNMS mass spectra, a previously-described double pulsing ion-extraction scheme[22] is used with a repetition rate of 2500 Hz to minimize surface charging effects and to suppress secondary ion

signals. Unless otherwise noted, the majority of prompt secondary ions are extracted by the first -2000 V pulse, of 1.15 μs duration, the end of which coincides (within ~0.1 μs) with the surface impact of the last of the primary ions (50 ns primary ion pulse width). Most of the sputtered neutrals have not yet interacted with the VUV beam during the application of the first extraction pulse. These neutrals are photoionized in the extraction region for 0.55 μs while the extraction potential is zero, until the second -2000 V extraction pulse of 5 μs duration is applied.

Despite the suppression of the SIMS ions under these extraction conditions, some secondary ions are still transmitted through the analyzer, necessitating the collection of three datasets: the synchrotron-only background, the residual SIMS background, and the total signals resulting from both the synchrotron and the Bi_3^+ ion beam together. The VUV-SNMS spectra presented in this paper are the result of the subtraction of both the synchrotron-only background and residual SIMS background from the total signal. Analyzer conditions for VUV-SNMS spectra (including the background scans) are optimized for the detection of photoionized neutrals, and no electrons are used to neutralize the surface, as sample charging is not observed.

The VUV spectral resolution at the beamline port used for VUV-SNMS is determined to be 0.2 eV by measuring the full width at half maximum of the autoionizing resonance of ion-sputtered silicon atoms at 9.8 eV.[22] Argon is used in the gas filter for all VUV-SNMS experiments, and a 100 μm horizontal slit in the gas filter is used to narrow the vertical height of the VUV beam. The resultant beam delivers ~10^{15} photons/s with a spot size of approximately 200 μm (vertical) × 600 μm (horizontal) to the photoionization interaction region. As in the TDMB experiments, VUV-SNMS PIE curves are normalized using photon flux curves determined using a NIST-calibrated photodiode.

Samples analyzed by SIMS and VUV-SNMS are prepared on silicon substrates (Wafer World, Inc.; P/N 1183) by directly depositing the monolignols onto the silicon and subsequently dissolving and dispersing the applied compound with high-purity (99.9%) methanol. Samples are allowed to air-dry. After the samples are introduced into the main chamber, they are cooled to -20 °C to suppress background signals from the photoionization of thermally evaporating monolignols. For this purpose, a heating-cooling (H/C) stage that is thermally coupled to a reservoir of liquid nitrogen is used. A thermocouple is placed under the silicon substrate to monitor the sample temperature, and the temperature is maintained at -20 °C by the SurfaceLab 6.1 software. Modified sample clamps are used with the H/C stage to permit the VUV light to pass as close as possible over the sample surface.

Calculations of Energetics

Calculations are performed to estimate the IEs and fragment AEs for comparison to experiment. Geometry optimization and vibrational frequency calculations of the neutral and ionic species and the main fragments for coniferyl alcohol are carried out using the Gaussian 03 program[32] at the B3LYP level with the 6-311++G(2df,2pd) basis set. The approximate initial geometry for coniferyl alcohol is taken from Wei et al.[33] Adiabatic IEs, including the zero point energy (ZPE) corrections, are obtained for the coniferyl alcohol parent and the m/z = 124, 137, 151, and 152 fragments from the difference of the computed energies of the optimized cations and neutral structures. 4-ethylguaiacol is used as a benchmark molecule. The calculated and measured TDMB IEs for 4-ethylguaiacol are 7.4 eV and 7.6 eV ± 0.1 eV, respectively.

Single-point MP2 calculations are performed for coniferyl alcohol with the same 6-311++G(2df,2pd) basis set on the B3LYP-optimized structures to improve the calculated IE so that it is 0.3 eV lower than the measured TDMB IE value. ZPEs for the neutral and cation structures of coniferyl alcohol are determined at the B3LYP level with the same basis set and are included in the final calculated value of the coniferyl alcohol IE.

In order to assist in the interpretation of the experimentally observed AEs of the coniferyl alcohol fragments, the difference between the energies of the parent cation and the optimized fragments (with ZPE corrections) are used to determine the minimal energy required for fragmentation. These differences are referred to as AEs throughout this paper. Minimal structural rearrangement is assumed when optimizing the geometry of the fragments; therefore the results are representative of local minima only. Higher-energy transition states and potential energy barriers are not considered in calculating these AEs. Due to the size of the molecules and the complexity of the potential energy surfaces, a unique identification of the transition pathways is not performed, as it is beyond the scope of this paper.

Results and Discussion

Thermal Desorption Molecular Beam Photoionization of Coniferyl Alcohol

Coniferyl alcohol is thermally desorbed at a series of nozzle temperatures (40 °C – 110 °C) and is ionized at 11 eV photon energy. Mass spectra acquired at several nozzle temperatures are shown in Figures 2a-2c. Between 40 °C and 50 °C, no signal is observed for the coniferyl alcohol parent ion at a mass-to-

charge ratio (m/z) of 180 (Figure 2a). At ~60 °C, the signal from the parent ion appears, and lower mass peaks (m/z = 124, 137 and 152) also grow in as the parent ion signal increases with increasing nozzle temperature (Figures 2b-2c). Scans over a larger mass range at 11 eV photon energy and 110 °C yield no evidence for features in the mass region of the coniferyl alcohol dimer within a parent signal-to-baseline ratio of 90. The peak at m/z = 181 also shows the expected intensity relative to the coniferyl alcohol parent mass from isotope distributions, which illustrates the negligible presence of protonated coniferyl alcohol that would arise from the fragmentation of coniferyl alcohol clusters.

In the lower-temperature spectra, the m/z = 152 feature is predominant. This signal decreases relative to the parent peak as the nozzle temperature is increased, and this decrease continues even when the nozzle is held at a constant temperature. This suggests that m/z =152 results from a contaminant, although it is possible that there is a small, underlying contribution to the m/z = 152 peak from the dissociative photoionization of the parent molecule. Drastic fluctuations in the intensity of m/z = 152 relative to the parent mass at m/z = 180 are observed when different bottles of coniferyl alcohol obtained from Alfa Aesar or Sigma Aldrich (all 98% purity) are used, which is indicative of accumulated degradation products from prolonged sample storage or from residual contaminants from synthesis. The m/z = 152 peak is assigned below to vanillin. Other characteristic fragments at m/z = 124 and 137 have signal intensities that exhibit constant ratios with respect to the parent peak with increasing nozzle temperature and are thus attributed to dissociative photoionization of the parent molecule.

After increasing the nozzle temperature to 110 °C to obtain workable signal counts, mass spectra are collected as a function of photon energy. Spectra of coniferyl alcohol at 9.1 eV, 12.1 eV and 15.1 eV are shown in Figures 2d-2f. The parent signal at m/z = 180 dominates below 9 eV and has a signal-to-baseline ratio of ~35, highlighting the capability of threshold single-photon ionization to obtain fragment-free mass spectra.[19,34] As the photon energy is increased, features at m/z = 124, 137, and 151 appear (Figures 2e-2f). The strongest lower m/z peaks appear at 18, 32 and 40, which correspond to H_2O, O_2 and argon, respectively. The presence of argon in the mass spectrum below its IE of 15.76 eV was discussed above.

The parent molecule is a prominent peak at all photon energies examined in the TDMB experiments, although dissociative photoionization increases at higher photon energies. At 9.1 eV, the ratio of the molecular parent signal intensity to the summed intensity of the main fragments is essentially infinite (here, m/z = 124 and 137 constitute the main fragments since the transient sample contaminant

dominates the contributions to m/z = 152 and 151), while at 12.1 eV and 15.1 eV, the parent-to main fragments ratio decreases to ~0.4 and ~0.2, respectively. The integrated peak intensity for coniferyl alcohol is plotted versus photon energy in Figure 3. By performing a linear fit to the low photon energy baseline and onset slope of the PIE curve, the IE is determined to be 7.60 eV ± 0.05 eV. This disagrees with the calculated results of ten Have *et al.*[35] who predict an IE of 8.60 eV ± 0.06 eV, but is in reasonable agreement with calculations by Wei *et al.*[33], who predict an IE of 7.26 eV, and with calculations in this work, which predict an adiabatic IE of 7.3 eV.

The major fragments of coniferyl alcohol observed with VUV photoionization are comparable to those observed in EI spectra, and the similarities increase with increasing photon energy. Previous structural assignments for fragments from EI[36] are used to decipher the fragmentation mechanism in this experiment. IEs and AEs for the proposed structures[36] are calculated and compared to the experimentally-determined AEs and previous theoretical IE values in Table 1. The structures involved in the various coniferyl alcohol fragmentation mechanisms considered here, together with their sinapyl alcohol analogues, are shown in Figure 4. The photoionization of vanillin and 4-ethylguaiacol are also included in the figure as possible sources of the m/z = 152 contaminant.

In EI spectra, m/z = 152 is assigned to a five-member ring structure (Figure 4, Structure A cation),[36] arising from CO elimination from the ring structure. Due to the aforementioned decay of the m/z = 152 signal with respect to the parent in the TDMB experiments reported here, it is uncertain to what extent dissociative photoionization contributes to the m/z = 152 signal. Instead, it appears that the obtained appearance curve of m/z = 152 is dominated by the ionization of a transient degradation product or contaminant.

4-ethylguaiacol, an observed thermolysis product of coniferyl alcohol,[37] and vanillin, a pyrolysis product found in dehydrogenation lignin polymers and milled wood lignin[8] are two possibilities for m/z = 152. The TDMB AE of m/z = 152 is 8.3 eV ± 0.2 eV. The IEs of neutral 4-ethylguaiacol (7.6 eV ± 0.1 eV, this work) and vanillin (8.30 eV ± 0.05 eV)[38] are included in Table 1 for comparison. Based on these values, vanillin is determined to be the most likely source of m/z = 152 in the TDMB spectra. TDMB experiments are performed for pure vanillin to verify this assignment, and the resulting PIE curve and IE (8.30 eV ± 0.05 eV, this work) agree with the appearance curve and AE of m/z = 152 in the coniferyl alcohol TDMB spectrum (Figure 5a).

In a previous EI analysis, m/z = 151 has been assigned to the cation of Structure B, a fragment of the five-member ring m/z = 152 (Structure A) cation.[36] While this structural assignment has at most a minimal contribution to the signals observed in these experiments, the concurrent decay of m/z = 151 with m/z = 152 over time indicate that m/z = 151 is related to the m/z = 152 peak. From the shape of the two appearance curves (Figure 5b) it can be seen that the m/z = 152 (vanillin) signal intensity plateaus after 11.8 eV, which coincides roughly with the onset of the m/z = 151 signal at 11.5 eV. This implies that m/z = 151 arises from the fragmentation and depletion of vanillin, thus making the vanillin – H cation the most likely assignment (Structure C cation). This assignment is further supported by the similar appearance curve of m/z = 151 observed in the TDMB spectra of pure vanillin (data not shown). This vanillin – H structural assignment has also been previously made for m/z = 151 in SIMS spectra.[12]

The fragment at m/z = 137 has been attributed to the molecular rearrangement of the parent ion and subsequent loss of a neutral radical CH_2CHO in the EI[36] and SIMS[12] mass spectra (Structure D cation). In the TDMB experiments, the m/z = 137 cation has an experimental AE of 10.35 eV ± 0.05 eV. The calculated IE (6.5 eV) of the optimized neutral structure for m/z = 137 is much lower than the observed AE at this mass, and there is no evidence, within the signal-to-noise, of the co-fragment at m/z = 43; hence the 137 mass fragment is attributed to dissociative photoionization of the parent molecule.

A calculated AE for the dissociative ionization that leads to the m/z 137 cation was explored theoretically. The calculated AE for the optimized m/z = 137 cation structure and its corresponding neutral radical CH_2CHO fragment is 8.9 eV. This is lower than the experimental TDMB AE, indicative of the presence of higher energy barrier(s) involved in the fragmentation, a feasible scenario given that the neutral parent molecule must undergo rearrangement of two of its hydrogen atoms before fragmentation. A detailed theoretical mapping of the dissociation pathway is outside the scope of the current work.

The fragment at m/z = 124 is assigned to the guaiacol cation, which has an experimentally-observed TDMB AE of 10.50 eV ± 0.05 eV. This AE is much higher than is expected for direct ionization of neutral guaiacol, calculated by Wei et al[33] and also in the present paper (7.95 eV and 7.7 eV, respectively). This disparity and the absence of ion signal from the complementary neutral C_3H_4O fragment at m/z = 56 provide evidence that the observed guaiacol ion signal arises from the dissociative photoionization of coniferyl alcohol.

As was noted, the complementary neutral fragment for the guaiacol cation has a mass of 56 amu. While this mass may correspond to several different structures, propargyl alcohol and 2-propenal are considered as the two most feasible possibilities since they require the least amount of atomic rearrangement during the dissociation process. Calculation of the AE for the guaiacol cation with these two possible m/z = 56 neutral fragments shows that the propargyl alcohol is the more likely co-fragment (see Table 1), with a calculated AE of 9.6 eV, compared to 8.2 eV for the 2-propenal.

Thermal Desorption Molecular Beam Photoionization of Sinapyl Alcohol

Sinapyl alcohol is similar to coniferyl alcohol in structure, differing only by an additional $–OCH_3$ group that replaces a hydrogen on the aromatic ring (Figure 1); therefore it shares many fragmentation patterns with coniferyl alcohol, resulting in similar mass peaks shifted by 30 mass units, which is the difference in mass due to the OCH_3 group versus the H group.

During TDMB experiments, the nozzle temperature is varied from 40 °C to 140 °C, and photoionization is observed with 11 eV photons. The parent ion (m/z = 210) appears concurrently with dihydrosinapyl alcohol (m/z = 212) and high mass fragments from both species (m/z = 154, 167, 168, 181, 182) when the nozzle temperature reaches approximately 65 °C. Similar to coniferyl alcohol, TDMB mass spectra collected over a larger mass range at 10 eV photon energy and 140 °C show no peaks in the dimer mass region within a parent signal-to-baseline ratio of 75, and the peak at m/z = 211 shows the expected intensity with respect to the m/z = 210 from natural isotopic distributions; hence fragment peaks are assumed to arise from the monomer and any contaminants within the sample, and not from clusters of sinapyl alcohol.

Select spectra at different photon energies are shown in Figure 6. As with coniferyl alcohol, sinapyl alcohol TDMB mass spectra at low photon energies below 9 eV (Figure 6a) are essentially fragment free (dihydrosinapyl alcohol, a common contaminant in syntheses of sinapyl alcohol[39], and its fragments are ignored). The parent signal persists at all photon energies investigated in this study, even as dissociative photoionization becomes more dominant. At 9 eV, the ratio of the molecular parent signal intensity to the summed intensity of the main fragments is essentially infinite (here, m/z = 154, 167, and 182 constitute the definitive main fragments; m/z = 181 could not be confirmed to originate from sinapyl alcohol), while at 12 eV and 15 eV, the parent-to main fragments ratio decreases to ~0.8 and ~0.3, respectively.

The peaks at m/z = 18 and 32 (Figures 6b-6c) are assigned to H_2O and O_2; this assignment is confirmed by the observed IEs, which agree well with literature values.[40,41] The m/z = 212 peak, seen in Figures 6a-6c is attributed to the presence of unsaturated dihydrosinapyl alcohol, which is a common contaminant in syntheses of sinapyl alcohol.[39] As with coniferyl alcohol, the peak at m/z = 40 corresponds to ionization of argon, and the low molecular weight co-fragments of m/z = 182, 167 and 154 (m/z = 28, 43, and 56) are notably absent even at 15 eV (Figure 6c). This suggests that the heavier mass fragments arise from dissociative photoionization of either sinapyl alcohol or the dihydrosinapyl alcohol contaminant.

Figure 7a shows the PIE of sinapyl alcohol, from which an adiabatic IE of <7.4 eV is determined. The lowest available photon energy at the beamline is 7.4 eV, however the IE can be estimated further by extrapolating the PIE curve to a zero baseline. A zero baseline is regularly achieved at the monochromatized light port on the beamline in the low photon energy range since few background gas species are ionized at these energies. Such an extrapolation yields an estimated sinapyl alcohol IE of 7.35 eV. With the lack of a measurable baseline, error bars for this value cannot exactly be determined, but it can likely be safely assumed that the IE values are correct within 0.5 eV. A similar extrapolation is used to determine the IE of dihydrosinapyl alcohol to be 7.30 eV (Figure 7b).

The mass m/z = 182 is attributed to the loss of a carbon and oxygen atom, one possible resultant structure being 4-ethylsyringol. This peak increases with the sinapyl alcohol signal (m/z = 210) as the nozzle temperature is increased, consistent with a constant-fraction dissociative photoionization product of sinapyl alcohol. This correlative dependence on the parent molecule is in contrast to the distinctly different behavior of vanillin (m/z = 152) in the case of coniferyl alcohol.

Structure E (m/z = 167) appears at about 1.3 eV higher in photon energy than the corresponding m/z = 137 from coniferyl alcohol, which may be due to a higher activation energy associated with the prerequisite rearrangement of the alcohol tail in the sinapyl alcohol molecule. The m/z = 167 mass peak is also accompanied by a mass peak at m/z = 168. This latter peak is assigned to 4-methylsyringol, which likely arises from hydrogen rearrangement and loss of C_2H_4O from the non-negligible amounts of the contaminant dihydrosinapyl alcohol. This conclusion is supported by the temperature dependence of the m/z = 168 peak intensity, which varies with the signal intensity of dihydrosinapyl alcohol (data not shown).

The syringol cation is the tentative assignment of the m/z = 154 peak in the sinapyl alcohol mass spectrum. Syringol has an experimental AE of 11.00 eV ± 0.05 eV, which is about 0.5 eV higher than the AE of guaiacol (m/z = 124) from coniferyl alcohol. Syringol arises from sinapyl alcohol via the loss of the long alcohol tail and a hydrogen donation to the charged fragment.

Both coniferyl alcohol and sinapyl alcohol exhibit fragment-free TDMB photoionization mass spectra at low photon energies (*e.g.* below 9 eV) and exhibit characteristic dissociative ionization fragments at higher photon energies, although the parent masses remain clearly observable at all photon energies used. As will be seen in the next section, these same signature fragments are also observed in the VUV-SNMS mass spectra. The analysis of the TDMB experiments is therefore fully applicable for a thorough understanding of the origins of the mass spectral features in VUV-SNMS.

Secondary Ion and Secondary Neutral Mass Spectrometry (SIMS and SNMS) of Coniferyl Alcohol

Secondary ion and secondary neutral mass spectra are collected from Bi_3^+ ion sputtering of coniferyl alcohol deposited onto silicon substrates. Figure 8 presents comprehensive mass spectral results for SIMS ions, the TDMB data taken on the other apparatus, and VUV-SNMS analyses, the latter two at two different photon energies around 9 eV and 15 eV. The SIMS data (Figure 8a) reproduces the main SIMS signatures published previously.[12] The m/z = 137 feature has been tentatively assigned to the cation fragment $C_8H_9O_2^+$ (Structure D), and the m/z = 151 feature has been assigned mainly to the $C_8H_7O_3^+$ fragment (Structure C).[12] Figure 8a illustrates the great complexity of the SIMS spectrum, compared to the TDMB spectra presented in Figures 8b-8c.

Qualitatively, the VUV-SNMS mass spectra are simpler than the corresponding SIMS spectra, although they share similar spectral features with both SIMS and TDMB mass spectra. As can be seen in Figure 8a, the SIMS spectrum shows only a few strong characteristic fragments at m/z = 137 and 151, along with a huge array of other masses, while the VUV-SNMS spectra (Figures 8d-8e) show clear characteristic peaks at m/z = 124, 137, 151 and 180, similar to the TDMB experiments (Figure 8b-8c). The m/z = 152 (*e.g.* vanillin) peak does not appear as a major fragment in VUV-SNMS spectra, which may be a result of the rapid energy input from the ion beam (and subsequently reduced degradation compared to the long exposure periods to high temperature in the nozzle region of the TDMB experiments).

The presence of several common fragments in the VUV-SNMS and TDMB experiments may be indicative of dissociative photoionization of the ion-sputtered parent molecules; however it is also likely that the

VUV-SNMS spectra have contributions from other sources, including the ionization of sputtered neutral fragments or released surface reaction products. While dissociative photoionization can be minimized by reducing the photon energy used to ionize the molecules, possible gas-phase neutral fragments can lead to an unavoidable source of fragment ions, since they arise from the initial ion impact. Such mechanisms are likely responsible for the clusters of peaks in the coniferyl alcohol VUV-SNMS spectra in the regions around m/z = 150 and 165, which are also visible in the SIMS spectra, but are completely absent in the TDMB mass spectra even at 15 eV.

The prominent m/z = 28 peak in the VUV-SNMS mass spectrum at 15 eV (Figure 8e) is one such VUV-SNMS feature that does not arise from dissociative photoionization of the molecular parent. It is most likely due to CO and provides a simple starting point for evaluating the relative contributions of different sources of neutrals. This mass peak is not present in the TDMB experiments on coniferyl alcohol, and hence the CO cation is not believed to arise from dissociative photoionization of the coniferyl alcohol parent at the photon energies used. The observed CO also cannot be attributed to the ionization of any background gas by the synchrotron beam.

Although it is tempting to suggest that the photoionized CO may arise from neutral CO desorbed directly from the surface, there are other possible sources that must be considered. The neutral CO may be a co-fragment of a secondary fragment ion, a co-fragment of another neutral fragment, or a product of a more complex process. To partly distinguish between the many possibilities, a brief estimate is performed. The CO photoionization cross section at 14.9 eV is ~15.3 Mb (1 Mb = 1 x 10^{-18} cm^2).[42] This photoionization cross section, the observed CO signal counts in the VUV-SNMS mass spectra at 15 eV, and the synchrotron flux at 15 eV can be used to estimate the number of neutral CO molecules being desorbed using the relation:[23]

$$N \approx \frac{Z}{0.08 \cdot \sigma F \tau}, \quad (1)$$

where N is the number of neutral CO molecules being desorbed from the surface, Z is the number of CO ions that are observed, σ is the CO photoionization cross section at 15 eV, F is the photon flux, and τ is the time that the desorbed CO molecules take to traverse the height of the ionizing beam (approximately 0.2 μs).[23] The calculated number of desorbed CO molecules is approximately five orders of magnitude larger than the total observed secondary ion counts at the same Bi_3^+ flux. This indicates that the amount of neutral CO observed cannot arise as a complementary fragment to the m/z = 151

and 152 (or other) secondary ions formed during the desorption event. The majority of neutral CO may be produced from larger neutral fragments or may be sputtered from a chemically modified surface (among other mechanisms). Distinguishing between the remaining possible sources of neutral CO is difficult since many parameters such as the ionization cross sections for m/z = 152, 151, and other possible species involved are unknown; however from the presence of released CO it is clear that dissociative photoionization of parent molecules is not the only process contributing to VUV-SNMS signals; other complex processes complicate the VUV-SNMS mass spectra compared to TDMB mass spectra.

Despite this possible limitation on the potential simplicity of the VUV-SNMS spectra of coniferyl alcohol, the parent mass at m/z = 180 is one of the major peaks in the VUV-SNMS spectrum. This contrasts with the corresponding SIMS spectrum, where m/z = 180 is just one of a number of mass peaks near the parent mass. By scanning the ionizing photon energy in coarse steps, a rough PIE curve is obtained for the ion-sputtered parent molecules at this mass. Relatively large energy spacing between data points is used due to the rapid decay of VUV-SNMS signal from the accumulation of ion-induced chemical damage of the sample during analysis. The VUV-SNMS PIE curve for coniferyl alcohol (Figure 9a) has an ionization onset of 8.0 eV ± 0.5 eV, where the uncertainty corresponds to the largest step size of the three averaged VUV energy scans. Within the error bars, this AE does match the IE of coniferyl alcohol obtained in the TDMB experiments (7.60 eV ± 0.05 eV). It may be thought that the ion desorbed species would harbor considerable internal energy and thus would have a lower IE, however it has been found that additional internal energy can have minimal effect on the absorption cross section and resulting IE for a neutral parent molecule in certain cases.[34]

Unlike the VUV-SNMS AE of the coniferyl alcohol parent, those of the fragments at m/z = 151 (loss of CO + H), m/z = 137 (loss of radical CH_2CHO), and m/z = 124 (guaiacol) are definitely shifted to lower photon energies compared to the TDMB experiments (see Table 1, Figures 9b-9d). This shift is apparent even with the relatively coarse photon energy steps, and it may be due to direct photoionization of ion-sputtered neutral fragments or the dissociative photoionization of vibrationally excited parent molecules. These two possibilities are considered below.

The m/z = 151 peak in the coniferyl alcohol VUV-SNMS spectra has an AE of 8.3 eV ± 0.5 eV (Figure 9b). The relatively high signal below 7.9 eV of the PIE curve is attributed to ionization from second harmonic radiation from the undulator, which passes through the argon-filled gas filter at lower photon energies. This baseline is not present in the TDMB data since krypton was used in the gas filter for those

experiments. Since VUV-SNMS analysis does not expose the sample to high temperatures for prolonged periods of time and is performed with a much lower chamber pressure than in the TDMB experiments, it is possible that the m/z = 151 observed in VUV-SNMS is not derived from the same transient species observed in the TDMB experiments (previously assigned to vanillin – H).

The observed VUV-SNMS AE for the coniferyl alcohol m/z = 151 lies 1.7 eV above the calculated IE of the optimized five-member ring neutral structure (Structure B)[36] resulting from CO and H loss, and over 2 eV below either the calculated or experimental (TDMB) AEs. The differences of these values compared to the AEs predicted for dissociative photoionization can be justified by the 2 eV to 2.5 eV of internal energy that is likely deposited into the neutral molecule during the ion sputtering event[22]. This reduces the energy needed from the ionizing photon to fragment the molecule, resulting in a lower AE for the ion-sputtered fragment. By the same reasoning, the dissociative photoionization of vanillin – H may also contribute, although its TDMB AE has a larger difference of 3.5 eV with the VUV-SNMS m/z = 151 AE. 4-ethylguaiacol does not exhibit a fragment at m/z = 151 in TDMB experiments of pure 4-ethylguaiacol (data not shown), so the VUV-SNMS signal does not arise from dissociative photoionization of 4-ethylguaiacol. The direct photoionization of neutral vanillin – H (Structure C) and 4-ethylguaiacol – H are further possibilities that cannot be eliminated.

The m/z = 137 in the VUV-SNMS spectra has an AE of 8.2 eV ± 0.5 eV (Figure 9c), which is about 2.2 eV lower than the AE in the TDMB experiments (10.35 eV). The calculated IE of neutral m/z = 137 (Structure D) is 6.5 eV. Since the AE is much higher than the calculated IE for Structure D, the m/z = 137 signal in the VUV-SNMS spectra is attributed to the dissociative photoionization of internally excited neutral parent molecules.

Guaiacol (m/z = 124) in the VUV-SNMS spectra has an AE of 8.4 eV ± 0.5 eV (Figure 9d), which is over 2 eV lower than the corresponding AE observed in the TDMB experiments (10.50 eV). The lowered AE may be due to internal energy imparted to coniferyl alcohol during the sputtering event or from the direct ionization of sputtered neutral guaiacol. The VUV-SNMS AE of guaiacol cannot rule out the latter possibility because, within error bars, photoionization of ion-sputtered neutral guaiacol (theoretical IE = 7.7 eV in this work, or 7.95 eV;[33] experimental IE = 8.0 eV[38]) is consistent with the VUV-SNMS AE.

The presence of common fragments between the coniferyl alcohol VUV-SNMS mass spectra and TDMB mass spectra imply that dissociative photoionization of intact sputtered neutral coniferyl alcohol molecules are the main source of fragmentation in the VUV-SNMS mass spectra. Although more

complex surface processes undoubtedly contribute to these spectra due to the high-energy primary ions involved, dissociative photoionization cannot be eliminated as an explanation for the formation of either m/z = 151 or guaiacol (m/z = 124) in the VUV-SNMS spectra. Dissociative photoionization is also the most likely mechanism for the appearance of m/z = 137 in VUV-SNMS.

Secondary Ion and Secondary Neutral Mass Spectrometry (SIMS and SNMS) of Sinapyl Alcohol

The SIMS, TDMB and VUV-SNMS spectra of sinapyl alcohol are shown in Figure 10. The VUV-SNMS spectra show significantly more SIMS-like character than coniferyl alcohol, as is evident by the many small peaks in the spectral baseline in Figure 10d. This increased neutral fragmentation may be due to the higher number of fragments possible for sinapyl alcohol due to its higher complexity and from the destabilizing effect of the additional OCH_3 group that is substituted for an H on the aromatic ring. It may also be due to the overlay of fragments from sample contaminants such as dihydrosinapyl alcohol due to the lower (80%) sample purity. Despite these complications, the sinapyl alcohol mass spectrum also exhibits the characteristic peaks observed in the TDMB photoionization experiments, including the molecular parent.

VUV-SNMS Probing of Cooler Molecules with Increased Extraction Delay

VUV-SNMS spectra of coniferyl alcohol at 9 eV are collected with several different extraction time delays and shown in Figure 11. The quoted delay values correspond to the time from the end of the first extraction pulse that suppresses secondary ions formed by the Bi_3^+ pulse to the beginning of the second pulse. This time also corresponds (within ~0.1 μs) to the time between the end of the primary ion pulse and the beginning of the second extraction pulse. As can be seen from Figure 11, the parent-to-fragment ratio increases with increasing delay time until 2.85 μs, at which point the intensity of the lower mass fragments increase from the relatively large contribution of the incompletely subtracted secondary ion background. The decreased fragmentation with longer delay time is understandable since molecules with lower internal energy are expected to leave the surface with less kinetic energy.[43] Longer extraction delay thus preferentially extracts VUV-postionized neutrals with lower internal energy and correspondingly reduced amounts of dissociative photoionization. The effect of the extraction delay is fairly dramatic in the case of coniferyl alcohol, possibly due to the particular energies needed to fragment the parent molecule. From the TDMB data, it is observed that coniferyl alcohol starts to fragment into m/z = 137 with the additional input of ~2.75 eV over the coniferyl alcohol ionization

energy. This is comparable to the ~2.5 eV of internal energy that is deposited into the molecule from the ion sputtering event.[22]

VUV-SNMS Sensitivity and Improvements

The more predictable fragmentation patterns observed in VUV-SNMS provide a significant advantage over SIMS analysis, where the amount of useful information extracted is often limited by the interpretation of complicated mass spectra. VUV-SNMS also has the benefit of being a more quantitative technique due to the reduced matrix effects observed in ion-sputtered neutrals[23]; hence the relative abundances of a compound from spot to spot can be more readily determined. As was alluded to earlier, however, this simplification of data interpretability comes at the price of sensitivity. From the intensity scales in Figures 8 and 10, it can be seen that the typical signal counts of SIMS are 10-10^3 times more intense than those for VUV-SNMS. This diminished sensitivity stems from the limited synchrotron photon flux and from the fact that most of the (quasi-continuous) VUV photons arrive at a time that does not coincide with the desorption event. Improved suppression of secondary ions could reduce the extraction delay necessary for the current double pulsing scheme, thus increasing VUV-SNMS signal intensities. Other future improvements to the sensitivity may arise by enhancing neutral desorption yields or by performing photoionization with a higher peak power, next generation light source.[44]

Conclusion

Coniferyl alcohol is studied in detail using single photon ionization with TDMB, VUV-SNMS and SIMS. The IE of coniferyl alcohol is measured to be 7.6 eV ± 0.05 eV. Sinapyl alcohol is also briefly investigated, and the IEs of sinapyl and dihydrosinapyl alcohols are both <7.4 eV. Fragments observed in the TDMB experiments are mainly the products of dissociative photoionization of the parent cation. M/z = 152 and 151 in the coniferyl alcohol sample arise from small amounts of vanillin within the sample. With these exceptions, the measured coniferyl alcohol fragment AEs are consistent with calculated AEs of optimized structures described in previously-postulated fragmentation mechanisms.[36]

The presence of CO in the coniferyl alcohol VUV-SNMS spectra indicates that the photoionization of released neutral gas-phase species as well as dissociative photoionization of sputtered parent molecules contribute to the VUV-SNMS signals of the monolignols. Mechanisms that lead to the release of neutral gas-phase fragments may account for the clusters of “SIMS-like” peaks in the VUV-SNMS spectra around

m/z = 150 and 165, since these peaks do not arise as dissociative photoionization products in the TDMB experiments. Such sources of neutrals may contribute to the VUV-SNMS spectra even when single-photon ionization is performed at threshold energies. CO formed as a co-fragment of positive secondary ion fragments contributes negligibly to the total CO observed.

Although it may not be possible to obtain completely fragment-free VUV-SNMS spectra, they are more straightforward to interpret compared to the corresponding SIMS spectra since VUV-SNMS have similar fragments as TDMB experiments. These shared fragments may be due to large contributions from dissociative photoionization of internally hot sputtered neutral parent molecules, and can be suppressed with the use of longer extraction delays, wherein the cooler populations of the desorbed neutral plume are sampled. Furthermore, the common peaks in the VUV-SNMS and TDMB experiments allow for the identification of characteristic mass markers for compounds of interest, thus improving the practical feasibility of more comprehensive chemical imaging studies of lignin and related compounds.

Acknowledgements

The authors would like to thank Corey Foster for his ongoing technical support of the TOF.SIMS V instrument. This work was supported by the Director, Office of Energy Research, Office of Basic Energy Sciences, and Chemical Sciences Division of the U.S. Department of Energy under contracts No. DE-AC02-05CH11231.

References

(1) Lin, Z.B.; Ma, Q.H.; Xu, Y. *Progr. Natur. Sci.* **2003**, *13*, 321

(2) Boerjan, W.; Ralph, J.; Baucher, M. *Annu. Rev. Plant Biol.* **2003**, *54*, 519.

(3) Hisano, H.; Nandakumar, R.; Wang, Z.-Y. *In Vitro Cell. Dev. Biol. Plant* **2009**, *45*, 306.

(4) Humphreys, J. M.; Chapple, C. *Curr. Opin. Plant Biol.* **2002**, *5*, 224.

(5) Schmidt, M.; Schwartzberg, A. M.; Perera, P. N.; Weber-Bargioni, A.; Carroll, A.; Sarkar, P.; Bosneaga, E.; Urban, J. J.; Song, J.; Balakshin, M. Y.; Capanema, E. A.; Auer, M.; Adams, P. D.; Chiang, V. L.; Schuck, P. J. *Planta* **2009**, *230*, 589.

(6) Bahng, M. K.; Mukarakate, C.; Robichaud, D. J.; Nimlos, M. R. *Anal. Chim. Acta* **2009**, *651*, 117.

(7) Reale, S.; Di Tullio, A.; Spreti, N.; De Angelis, F. *Mass Spectrom. Rev.* **2004**, *23*, 87.

(8) Izumi, A.; Kuroda, K. *Rapid Commun. Mass Spectrom.* **1997**, *11*, 1709.

(9) Streibel, T.; Fendt, A.; Geißler, R.; Kaisersberger, E.; Denner, T.; Zimmermann, R. *J. Therm. Anal. Calorim.* **2009**, *97*, 615.

(10) Tokareva, E. N.; Pranovich, A. V.; FardiM, P.; Danie, G.; Holmbom, B. *Holzforschung* **2007**, *61*, 647.

(11) Saito, K.; Kato, T.; Takamori, H.; Kishimoto, T.; Fukushima, K. *Biomacromolecules* **2005**, *6*, 2688.

(12) Saito, K.; Kato, T.; Tsuji, Y.; Fukushima, K. *Biomacromolecules* **2005**, *6*, 678.

(13) Kollmer, F.; Bourdos, N.; Kamischke, R.; Benninghoven, A. *Appl. Surf. Sci.* **2003**, *203-204*, 238.

(14) McLafferty, F. W.; Turecek, F. *Interpretation of Mass Spectra*, 4 ed.; University Science Books: Sausalito, CA, 1993.

(15) Wood, M.; Zhou, Y.; Brummel, C. L.; Winograd, N. *Anal. Chem.* **1994**, *66*, 2425.

(16) Wittig, A.; Arlinghaus, H. F.; Kriegeskotte, C.; Moss, R. L.; Appelman, K.; Schmid, K. W.; Sauerwein, W. A. G. *Mol. Cancer Ther.* **2008**, *7*, 1763.

(17) Müller, U.; Schittenhelm, M.; Schmittgens, R.; Helm, H. *Surf. Interface Anal.* **1999**, *27*, 904.

(18) Willingham, D.; Kucher, A.; Winograd, N. *Chem. Phys. Lett.* **2009**, *468*, 264.

(19) Mysak, E. R.; Wilson, K. R.; Jimenez-Cruz, M.; Ahmed, M.; Baer, T. *Anal. Chem.* **2005**, *77*, 5953.

(20) Cool, T. A.; Nakajima, K.; Mostefaoui, T. A.; Qi, F.; McIlroy, A.; Westmoreland, P. R.; Law, M. E.; Poisson, L.; Peterka, D. S.; Ahmed, M. *J. Chem. Phys.* **2003**, *119*, 8356.

(21) Streibel, T.; Geißler, R.; Saraji-Bozorgzad, M.; Sklorz, M.; Kaisersberger, E.; Denner, T.; Zimmermann, R. *J. Therm. Anal. Calorim.* **2009**, *96*, 795.

(22) Zhou, J.; Takahashi, L. K.; Wilson, K. R.; Leone, S. R.; Ahmed, M. *Anal. Chem.* **2010**, *82*, 3905.

(23) Takahashi, L. K.; Zhou, J.; Wilson, K. R.; Leone, S. R.; Ahmed, M. *J. Phys. Chem. A* **2009**, *113*, 4035.

(24) Freudenberg, K.; Neish, A. *Constitution and Biosynthesis of Lignin*; Springer-Verlag: Berlin, 1968.

(25) Nicolas, C.; Shu, J.; Peterka, D. S.; Hochlaf, M.; Poisson, L.; Leone, S. R.; Ahmed, M. *J. Am. Chem. Soc.* **2005**, *128*, 220.

(26) Belau, L.; Wilson, K. R.; Leone, S. R.; Ahmed, M. *J. Phys. Chem. A* **2007**, *111*, 7562.

(27) Amirav, A.; Even, U.; Jortner, J. *Chem. Phys.* **1980**, *51*, 31.

(28) Heimann, P. A.; Koike, M.; Hsu, C. W.; Blank, D.; Yang, X. M.; Suits, A. G.; Lee, Y. T.; Evans, M.; Ng, C. Y.; Flaim, C.; Padmore, H. A. *Rev. Sci. Instrum.* **1997**, *68*, 1945.

(29) Byrd, J. M. *Nucl. Instrum. Methods Phys. Res., Sect. A* **1999**, *427*, 614.

(30) Kaiser, R. I.; Maksyutenko, P.; Ennis, C.; Zhang, F.T.; Gu, X. B.; Krishtal, S. P.; Mebel, A. M.; Kostko, O.; Ahmed, M. *Faraday Discuss.* **2010**.

(31) Suits, A. G.; Heimann, P.; Yang, X.; Evans, M.; Hsu, C.-W.; Lu, K.-t.; Lee, Y. T.; Kung, A. H. *Rev. Sci. Instrum.* **1995**, *66*, 4841.

(32) Frisch, M. J., Trucks, G. W., Schlegel, H. B., Scuseria, G. E., Robb, M. A., Cheeseman, J. R., Montgomery, Jr., J. A., Vreven, T., Kudin, K. N., Burant, J. C., Millam, J. M., Iyengar, S. S., Tomasi, J., Barone, V., Mennucci, B., Cossi, M., Scalmani, G., Rega, N., Petersson, G. A., Nakatsuji, H., Hada, M., Ehara, M., Toyota, K., Fukuda, R., Hasegawa, J., Ishida, M., Nakajima, T., Honda, Y., Kitao, O., Nakai, H., Klene, M., Li, X., Knox, J. E., Hratchian, H. P., Cross, J. B., Bakken, V., Adamo, C., Jaramillo, J., Gomperts, R., Stratmann, R. E., Yazyev, O., Austin, A. J., Cammi, R., Pomelli, C., Ochterski, J. W., Ayala, P. Y., Morokuma, K., Voth, G. A., Salvador, P., Dannenberg, J. J., Zakrzewski, V. G., Dapprich, S., Daniels, A. D., Strain, M. C., Farkas, O., Malick, D. K., Rabuck, A. D., Raghavachari, K., Foresman, J. B., Ortiz, J. V., Cui, Q., Baboul, A. G., Clifford, S., Cioslowski, J., Stefanov, B. B., Liu, G., Liashenko, A., Piskorz, P., Komaromi, I., Martin, R. L., Fox, D. J., Keith, T., Al-Laham, M. A., Peng, C. Y., Nanayakkara, A., Challacombe, M., Gill, P. M. W., Johnson, B., Chen, W., Wong, M. W., Gonzalez, C., and Pople, J. A. Gaussian 03; Gaussian, Inc: Wallingford, CT, 2004.

(33) Wei, K.; Luo, S. W.; Fu, Y.; Liu, L.; Guo, Q. X. *J. Mol. Struc.-Theochem* **2004**, *712*, 197.

(34) Wilson, K. R.; Jimenez-Cruz, M.; Nicolas, C.; Belau, L.; Leone, S. R.; Ahmed, M. *J. Phys. Chem. A* **2005**, *110*, 2106.
(35) ten Have, R.; Rietjens, I. M. C. M.; Hartmans, S.; Swarts, H. J.; Field, J. A. *FEBS Lett.* **1998**, *430*, 390.
(36) Kovacik, V.; Skamla, J.; Joniak, D.; Kosikova, B. *Chem. Ber.* **1969**, *102*, 1513.
(37) Masuku, C. P. *J. Anal. Appl. Pyrolysis* **1992**, *23*, 195.
(38) Ponomarev, D. A.; Sergeev, Y. L. *Chem. Nat. Compd.* **1982**, *18*, 764.
(39) Kim, H.; Ralph, J. *J. Agric. Food Chem.* **2005**, *53*, 3693.
(40) Page, R. H.; Larkin, R. J.; Shen, Y. R.; Lee, Y. T. *J. Chem. Phys.* **1988**, *88*, 2249.
(41) Tonkyn, R. G.; Winniczek, J. W.; White, M. G. *Chem. Phys. Lett.* **1989**, *164*, 137.
(42) Cairns, R. B.; Samson, J. A. R. *J. Geophys. Res.* **1965**, *70*, 99.
(43) Chatterjee, R.; Postawa, Z.; Winograd, N.; Garrison, B. J. *J. Phys. Chem. B* **1999**, *103*, 151.
(44) Khan, S. *Journal of Modern Optics* **2008**, *55*, 3469

Table 1: Calculated and Experimental IEs and AEs

Errors next to each experimental IE and AE are based on the spectral resolution of the light and the size of the photon energy steps between data points. AEs are calculated assuming that the co-fragments are given by the chemical structures in parentheses. "—" indicates that theoretical or experimental values are either not available or not applicable to the given situation. All calculations in this work are performed at the B3LYP level except for the IE for coniferyl alcohol, which is calculated using MP2. All energies are in eV.

Main Fragment[a] (+cofragments)		IE of Main Fragment	Theoretical AE of Main Fragment Cation	TDMB AE	VUV-SNMS AE
Coniferyl Alcohol Sample					
Coniferyl Alcohol m / z = 180		8.60 ±0.06[d]; 7.26[e]; 7.3[b]	—	7.60±0.05	8.0±0.5
m / z = 152	Structure A (+CO)	6.8[b]	8.4[b]	—	—
	4-Ethylguaiacol	7.4[b]; 7.6±0.1[c]	—	—	—
	Vanillin	8.30±0.05[f]; 8.30±0.05[c]	—	8.3±0.2	—
m / z = 151	Structure B (+CO+H)	6.6[b]	11.0[b]	—	8.3±0.5
	Vanillin – H	—	—	11.5±0.2	
Structure D m / z = 137 (+·CH_2CHO)		6.5[b]	8.9[b]	10.35±0.05	8.2±0.5
Guaiacol m / z = 124	(+propargyl alcohol)	7.95[e]; 7.7[b]	9.6[b]	10.50±0.05	8.4±0.5
	(+2-propenal)		8.2[b]		
Sinapyl Alcohol Sample					
Dihydrosinapyl Alcohol m / z = 212		—	—	<7.4	—
m / z = 168 (+C_2H_4O)		—	—	10.80±0.05	—
Sinapyl Alcohol m/z = 210		7.10[e]	—	<7.4	—
m/z = 182 (+CO)		—	—	10.30±0.05	—
m/z = 181		—	—	10.8±0.2	—
m/z = 167 (+·CH_2CHO)		—	—	11.6±0.2	—
m/z = 154 (+C_3H_4O)		—	—	11.00±0.05	—

[a]Nominal mass; [b]Calculations from this work; [c]Evaluated from the TDMB PIE of the pure compound, this work; [d]Ref [35]; [e]Ref[33]; [f]Ref[38]

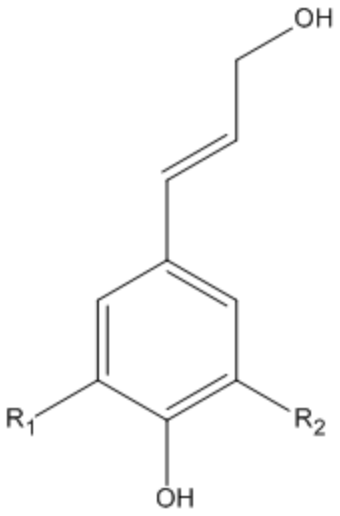

Coniferyl alcohol:
$R_1 = H, R_2 = OCH_3$

Sinapyl alcohol:
$R_1 = R_2 = OCH_3$

Figure 1: The molecular structures of coniferyl and sinapyl alcohol.

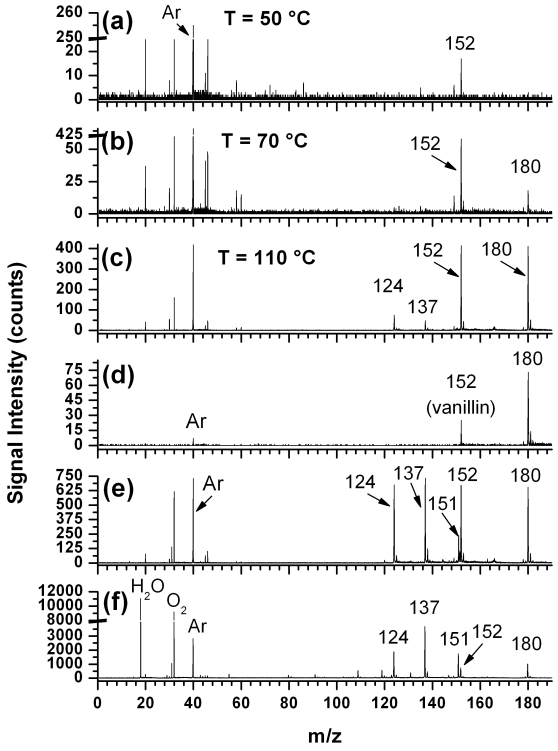

Figure 2: TDMB mass spectra of coniferyl alcohol collected with the nozzle at (a) 50 °C, (b) 70 °C and (c) 110 °C and photoionization at 11 eV. TDMB mass spectra for coniferyl alcohol at (d) 9.1 eV, (e) 12.1 eV and (f) 15.1 eV at a nozzle temperature of 110 °C.

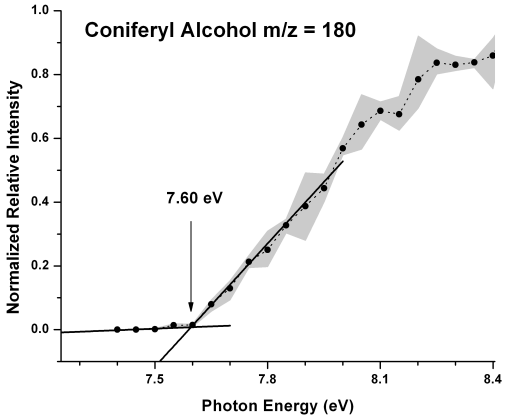

Figure 3: Signal intensity of coniferyl alcohol plotted versus ionizing photon energy. The extrapolation lines used for determining the AEs are in bold. Error bars are indicated by the gray shading. Adjacent data points are normalized with respect to each other with the measured photon flux curves.

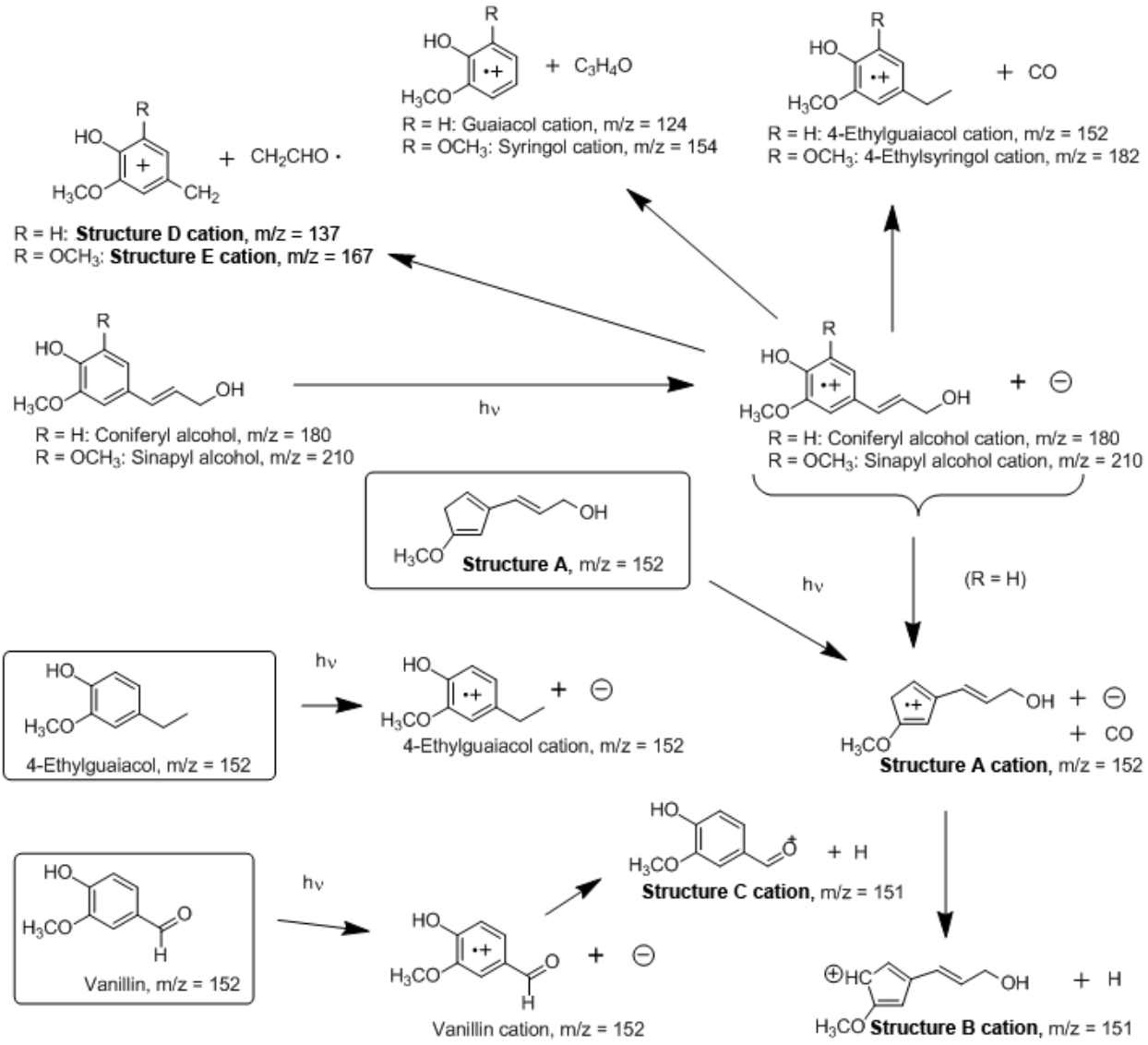

Figure 4: Diagram of the main fragmentation pathways examined in experiments on coniferyl alcohol (R = H). Possible contaminant or degradation products are indicated by the boxes. Sinapyl alcohol structural analogues (R = OCH_3) are also shown with their names.

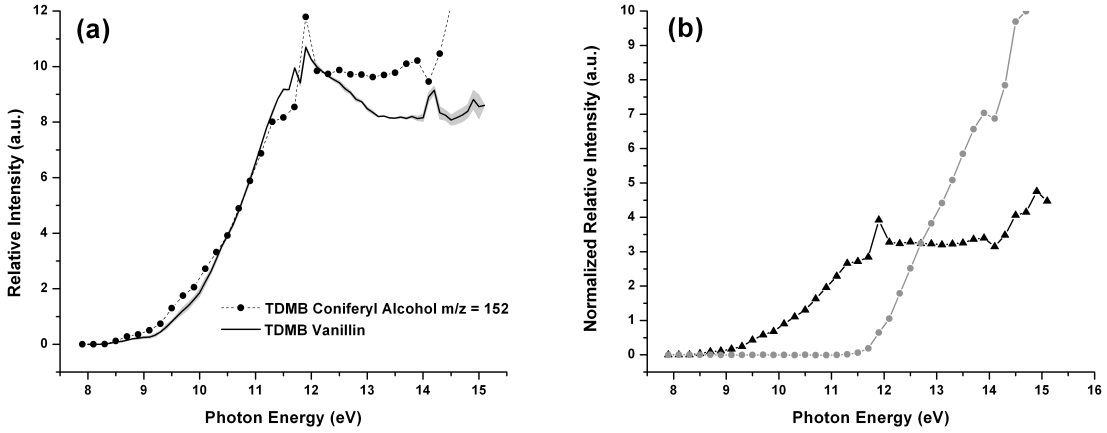

Figure 5: (a) Vanillin TDMB PIE (solid line) with error bars in gray and the TDMB appearance curve of m/z = 152 from the coniferyl alcohol spectrum (black circles with dashed line – larger photon energy step size). PIEs are normalized with respect to each other at 10.5 eV. Features near 12 eV and 14 eV arise from absorption lines of the argon in the gas filter. (b) Appearance curves of m/z = 151 (gray circles) and 152 (black triangles) from the coniferyl alcohol mass spectrum over a broad photon energy range. The two curves are scaled with respect to each other by an arbitrary factor for visual clarity.

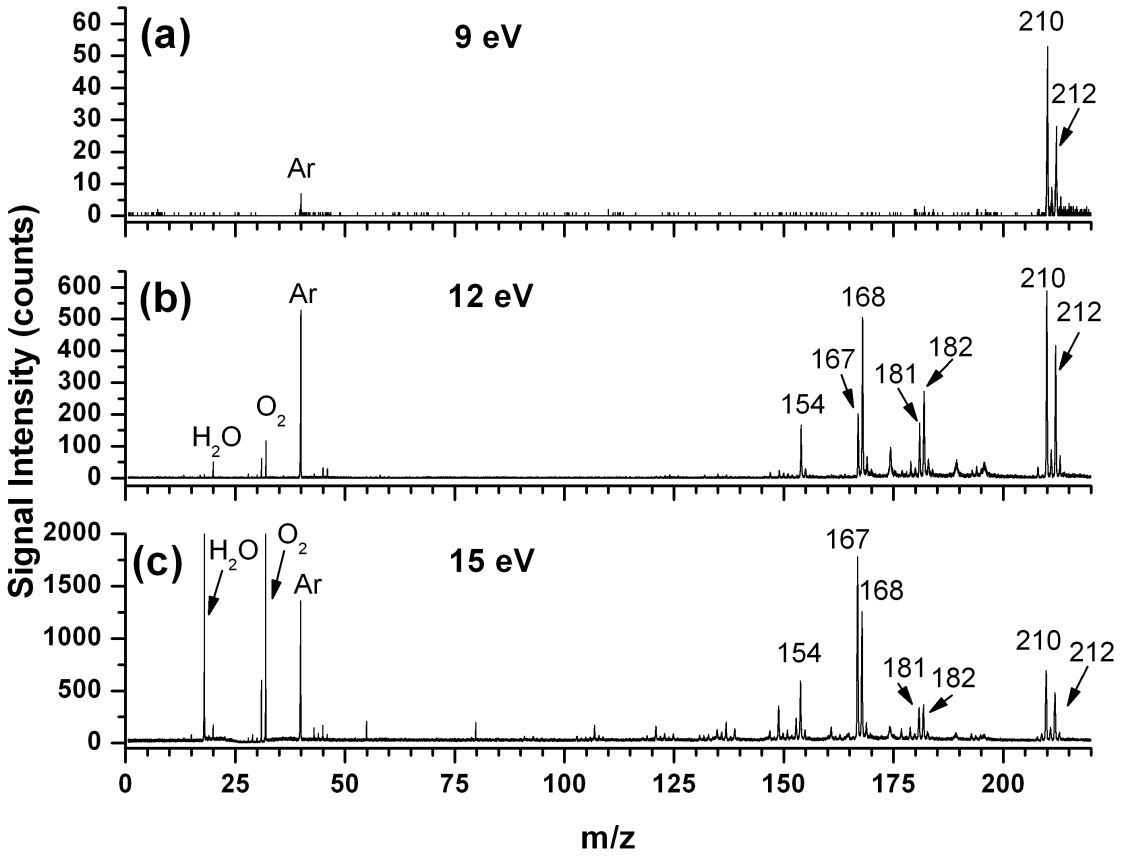

Figure 6: TDMB mass spectra of sinapyl alcohol at 140 °C and (a) 9 eV, (b) 12 eV and (c) 15 eV. M/z = 210 and 212 appear at approximately the same temperatures, but exhibit independent behavior with temperature.

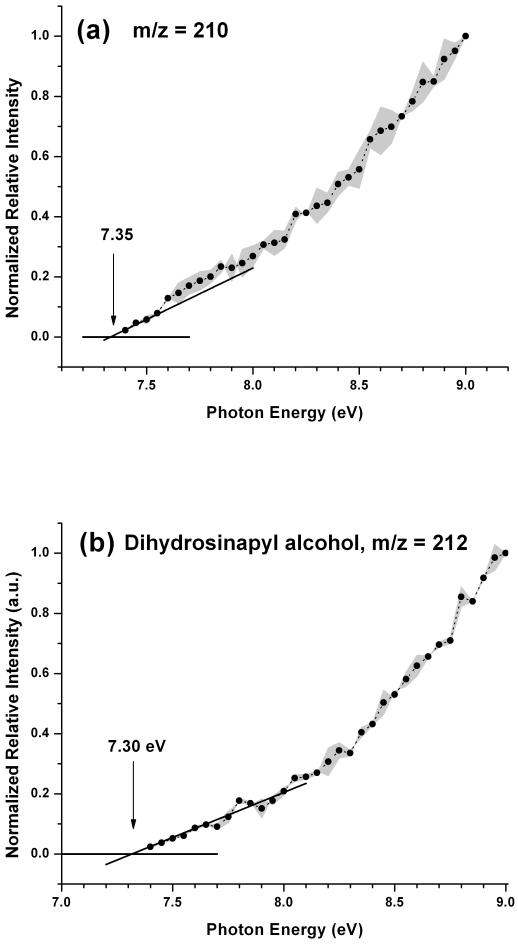

Figure 7: TDMB PIEs of (a) sinapyl alcohol and (b) dihydrosinapyl alcohol at a fixed nozzle temperature of 140 °C. Ionization onsets are estimated by extrapolating (bold lines) to a zero baseline.

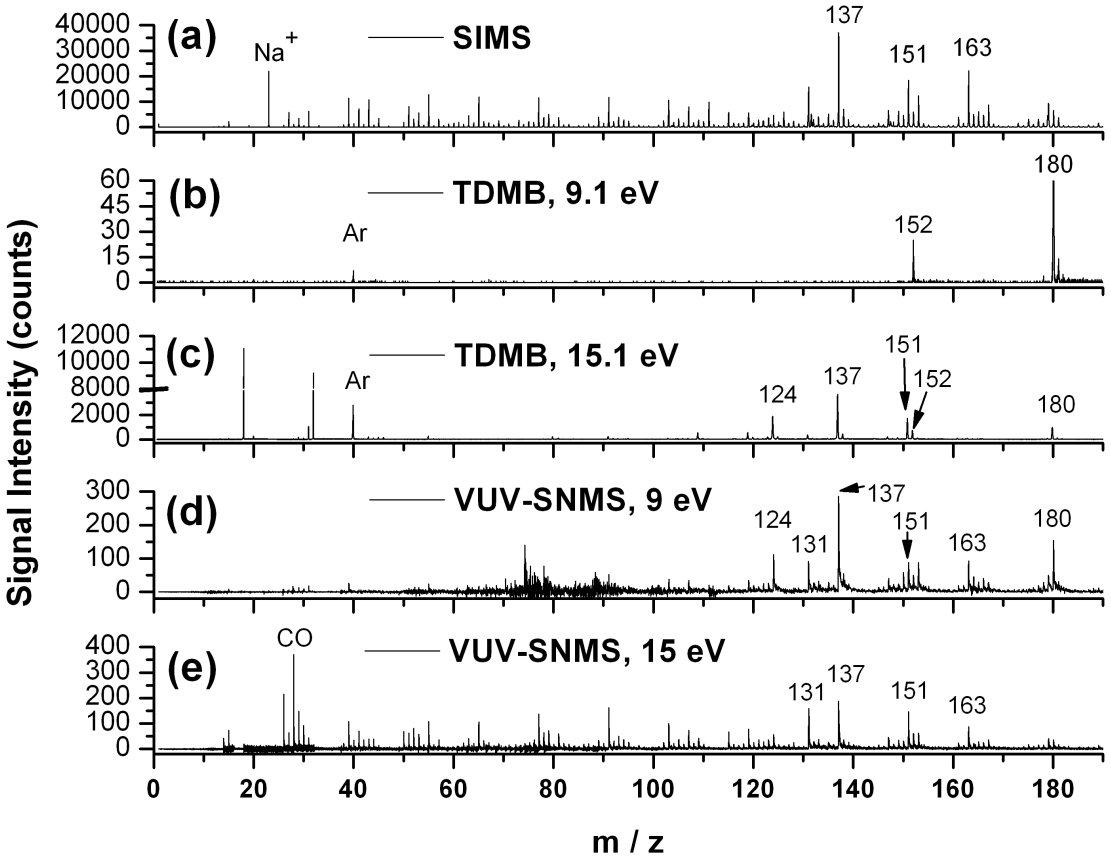

Figure 8: Comparison of coniferyl alcohol mass spectra obtained with (a) positive ion SIMS, TDMB at (b) 9.1 eV and (c) 15.1 eV, and VUV-SNMS at (d) 9 eV and (e) 15 eV. SIMS data is collected using 12.5 ns pulses of Bi_3^+ under analyzer conditions optimized for secondary ion detection.

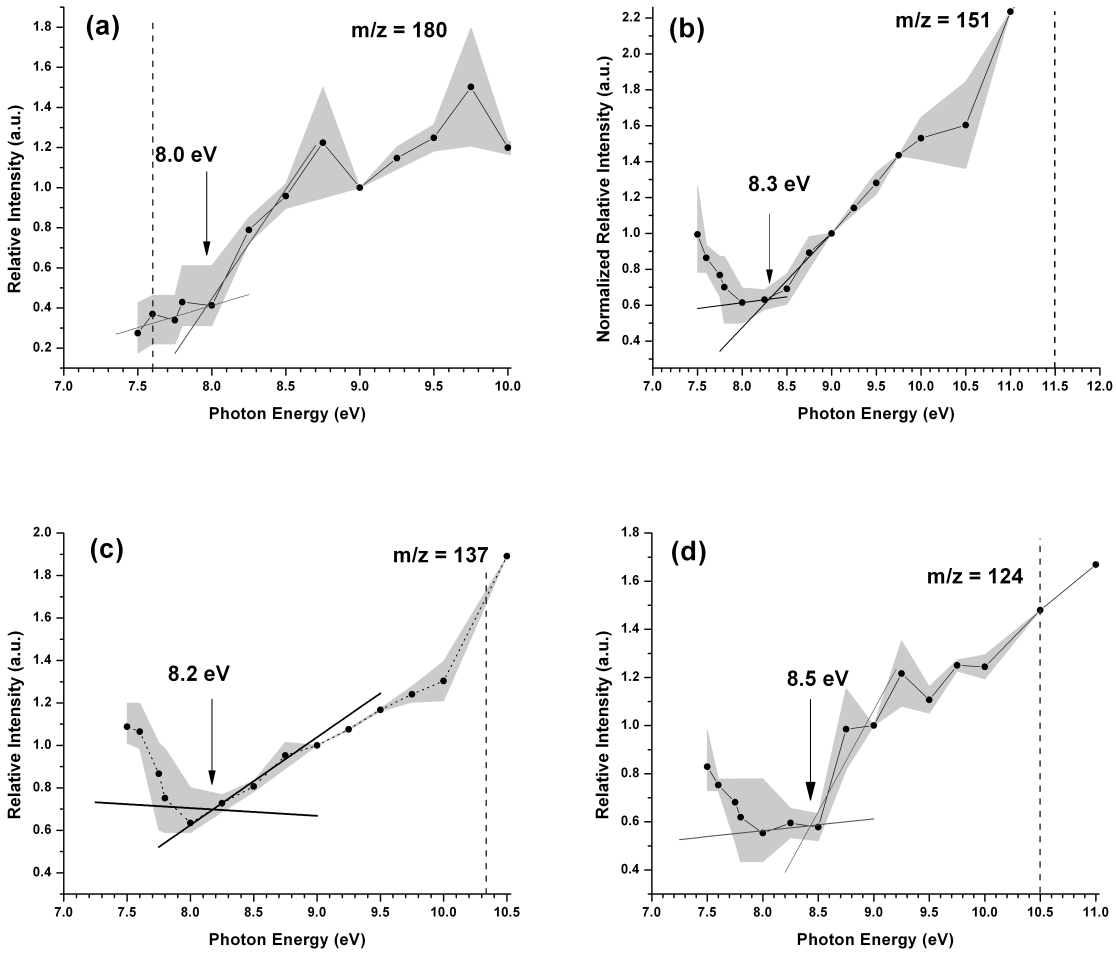

Figure 9: VUV-SNMS appearance curves for (a) coniferyl alcohol and the main VUV-SNMS fragments (b) m/z = 151, (c) m/z = 137 and (d) m/z = 124. The bold lines are the extrapolations, and the dashed vertical lines mark the ionization onsets observed in the TDMB experiments. Black circles represent averages of three datasets, collected at staggered photon energies and normalized with respect to each other at 9 eV. Error bars (gray shading) are determined for each point by linear interpolation of datasets. IEs are rounded to the nearest 0.1 eV.

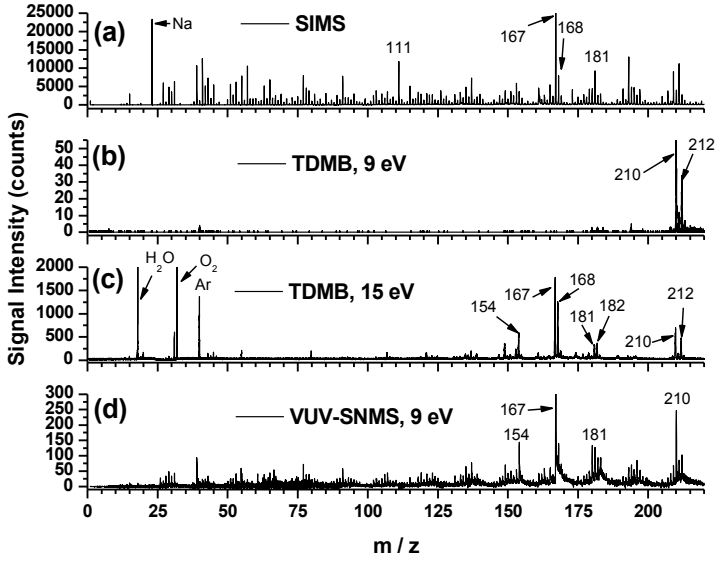

Figure 10: Mass spectra of sinapyl alcohol obtained using (a) positive ion SIMS, TDMB at (b) 9 eV and (c) 15 eV and (d) VUV-SNMS at 9 eV. SIMS data is collected using 12.5 ns of Bi_3^+ under analyzer conditions optimized for secondary ion detection. VUV-SNMS is obtained after the subtraction of background synchrotron and SIMS contributions. The feature at m/z = 111 in (a) is from a known contaminant in the spectrometer.

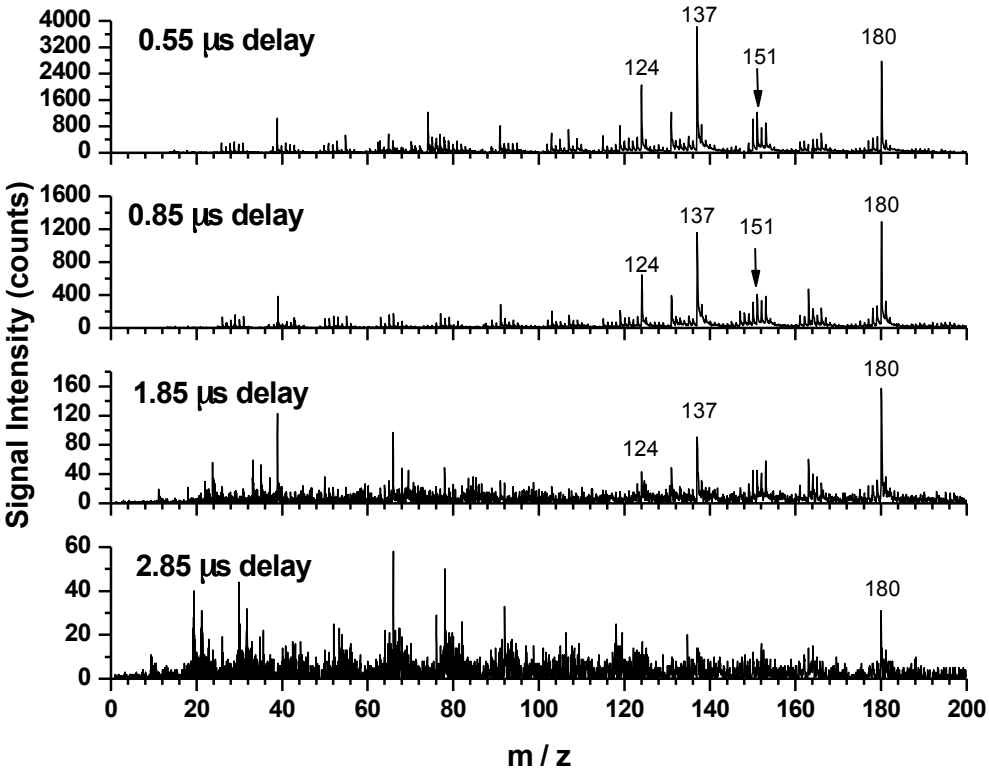

Figure 11: VUV-SNMS spectra of coniferyl alcohol at 9 eV, taken with increasing extraction delay. The parent-to-fragment ratio increases with increasing delay, until residual, background SIMS contributions dominate at 2.85 µs.